Palaeogeography, Palaeoclimatology, Palaeoecology (Global and Planetary Change Section), 98 (1992) 167–184
Elsevier Science Publishers B.V., Amsterdam

Hugo

Ground temperature histories in eastern and central Canada from geothermal measurements: evidence of climatic change

Hugo Beltrami [a], Alan M. Jessop [b] and Jean-Claude Mareschal [a,c]

[a] *GEOTOP, Université du Québec à Montréal, P.O. Box 8888, Station A, Montréal, Qué. H3C 3P8, Canada*
[b] *Institute of Sedimentary and Petroleum Geology, Geological Survey of Canada, 3303, 33rd Street, NW, Calgary, Alta. T2L 2A7, Canada*
[c] *Laboratoire de Dynamique de Systemes Géologiques, Institut de Physique du Globe, 4 Place Jussieu, Paris, Cedex 05, 75252, France*

(Received January 15, 1992; revised and accepted June 26, 1992)

ABSTRACT

Beltrami, H., Jessop, A.M. and Mareschal, J.-C., 1992. Ground temperature histories in eastern and central Canada from geothermal measurements: evidence of climatic change. Palaeogeogr., Palaeoclimatol., Palaeoecol. (Global Planet. Change Sect.), 98: 167–184.

Inverse and direct methods have been used to analyze a large number of borehole temperature logs in order to infer past climatic changes. Results indicate a warming of 1–2°C in eastern and central Canada during the past 150 years. A period of cooling between 500 and 200 years before present, corresponding to the time of the "Little Ice Age", has also been identified in the same areas. A regional ground temperature history is estimated for eastern and central Canada from the simultaneous inversion of several temperature logs. The inferred temperature changes appear correlated with the concentration of atmospheric carbon dioxide as reported from a Greenland ice core, and agree with existing meteorological and dendrochronological records for the area.

Introduction

Results from analyses of world-wide meteorological data (Hansen and Lebedeff, 1987; Jones et al., 1986) indicate a global average temperature increase of about 0.5°C in the last 100 years. However, meteorological records suffer from a number of shortcomings: uneven spatial distribution of measurements, variable standards, contamination by anthropogenic activities and reduced temporal length of records (Karl et al., 1989). Furthermore, recent works have questioned the significance of the results from these global studies, either in terms of the statistical significance of the inferred trends (Elsner and Tsonis, 1991), in the context of non-linear variability (Ghil and Vautard, 1991), or with respect to sampling biases (Willmott et al., 1991).

It has been shown that the geothermal measurements are affected by the past temperatures of the Earth's surface (Birch, 1948; Beck, 1977). Conversely, Vasseur et al. (1983) and Lachenbruch and Marshall (1986) have demonstrated that geothermal data can be used to extract the ground surface temperature history. The advantages of borehole temperature measurements rest mainly in the potential spatial coverage of measurements, the homogeneity of the data, and the fact that the Earth has filtered out high frequency temperature variations, recording only long-term trends. Disadvantages of these measurements include the decrease of resolution with depth and time, and the difficulties introduced by the many sources of noise which may produce a fictitious signal.

Correspondence to: H. Beltrami, GEOTOP, Université du Québec à Montréal, P.O. Box 8888, Station A, Montréal, Qué., H3C 3P8, Canada.

Throughout eastern and central Canada, the large majority of borehole temperature logs shows an attenuated or sometimes reversed temperature gradient near the surface with a minimum at depth of 60–100 m. There are many reasons for distortion of the conductive geothermal gradients, particularly near the surface, including conductivity contrast between soil and rock, water movement in unconsolidated material, proximity to sloping ground or bodies of water, recent human induced changes to the surface such as forest-clearing or urban development, rapid erosion and sedimentation, or changes in surface temperature (Chisholm and Chapman, 1992). The widespread nature of the observed temperature minimum suggests that, although local effects cannot be eliminated, there is some factor operating over a wide area.

This paper presents the results from inverse and direct analyses of about 200 borehole temperature profiles from central and eastern Canada. Ground temperature histories (GTHs) can be extracted from the temperature perturbations to the equilibrium geothermal gradient (routinely measured for heat flow density (HFD) determination). Although these GTHs do not automatically translate into an equivalent of the meteorological record, they do represent complementary information on climatic change since the subsurface temperature perturbation is determined, in these latitudes, mainly by long-term variations of surface air temperature and precipitation.

Results indicate, in all but three sites, an increase in ground temperature between 1–2°C in the last 150 years. From the deeper boreholes

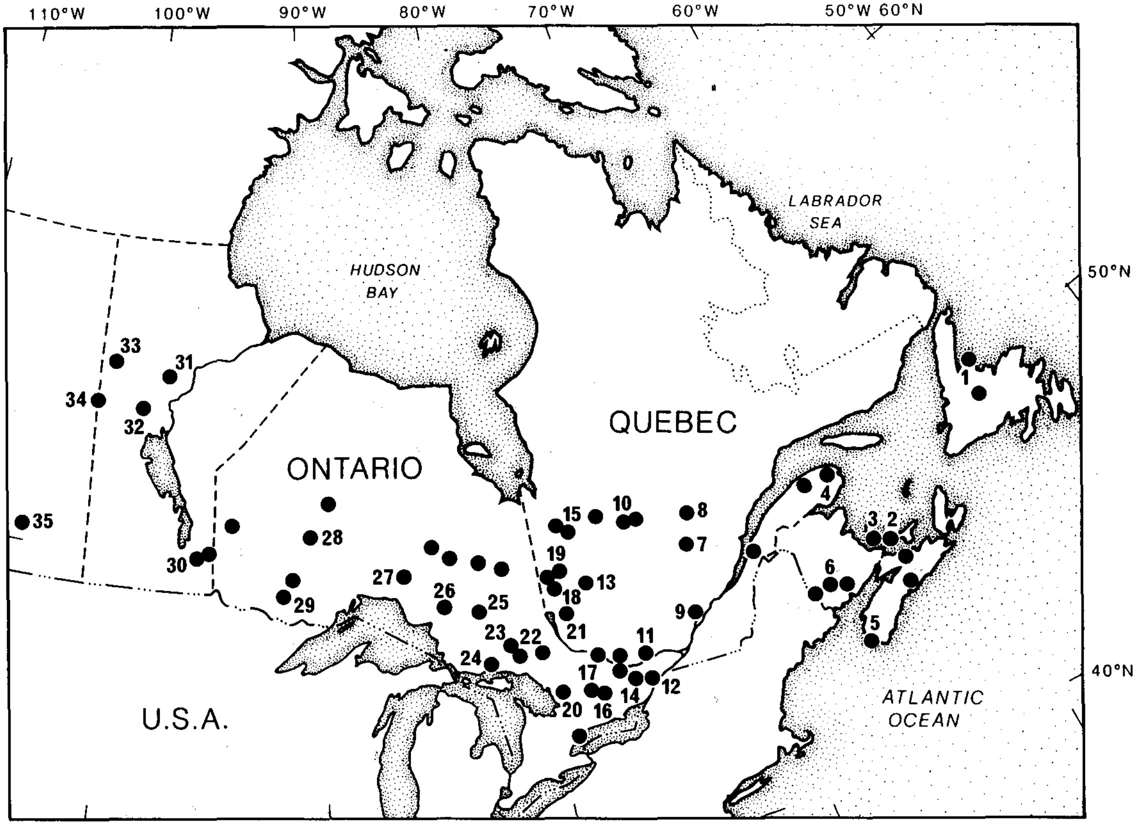

Fig. 1. Distribution of sites in central and eastern Canada. Dots mark the sites. The numbers correspond to the sites shown in Figs. 4, 5, and 7.

one can resolve, in most regions, a period of cooling between 500 and 200 years before present (yr B.P.) (−1°C) associated with the "Little Ice Age" (LIA). In this longer context, it is not possible to accurately isolate the part of the modern warming corresponding to anthropogenic activities over the last century from the natural climatic oscillations such as the LIA, although the magnitude of the post-industrial warming does exceed, in most areas, the cooling during the LIA. The warming detected is in agreement with meteorological and dendrochronological records (Archambault and Bergeron, 1992) for the area, and it is correlated with changes in atmospheric CO_2 concentration measured in a Greenland ice core (Wahlen et al., 1991).

Data

Two sets of borehole temperature data, covering an irregular area of about 2000 × 500 km, in southeastern and central Canada have been assembled. The distribution of the data in this region extending from Saskatchewan to Newfoundland is displayed in Fig. 1. The data distribution is irregular since the temperature measurements have, with a few exceptions, been carried out in holes of opportunity in regions of mining activity. The first data-set forms part of the geothermal database collected by the Geological Survey of Canada since 1965 (data-set G). The other data-set was collected by the University of Quebec at Montréal and the Institut de Physique du Globe at Paris (data-set Q).

The joint G and Q sets consist of more than 200 high-resolution temperature profiles, distributed among approximately 60 sites (depending on the site definition criteria). Data-set Q also contains a number of water–well temperature logs in the area of Lac St. Jean (Québec). These sites have been discussed by Pinet et al. (1991) with respect to landscape disruption in the area, and are not included in this study.

Temperature measurements were carried out using calibrated thermistors with an precision of about 2 mK with an estimated accuracy of 0.02 K considering the uncertainties in depth measurements. Thermal conductivity measurements are available for most of the boreholes, although not always in the upper-most section (0–200 m) of the borehole, where the temperature perturbations are usually found.

When thermal conductivity measurements are not numerous, the lithological logs have been consulted in order to infer potential large variations of thermal conductivity; if such variations do not appear likely, then an average value of the thermal conductivity has been used with the temperature log in question.

Several criteria have been used to select the final data-set to be analyzed and interpreted. Firstly, each temperature profile has been examined visually to identify obvious disturbances due to ground-water flow. Main candidates are the boreholes located on slopes or in narrow valleys. Boreholes located in or near urban centers have also been discarded since it is expected that the "natural" recent climatic signal would be masked by the urban heat island effect or by the disruption of the surface environment due to agricultural activity or construction. Furthermore, effects of topography have been taken into account in order to avoid biasing the results; care has been taken to discard boreholes located in south-facing and north-facing slopes (Blackwell et al., 1980). Boreholes located near or under bodies of water have not been used in the analysis since the effects of lateral heat conduction are not easily eliminated and often exceed the effect of recent surface warming. Finally, care has been taken to identify and avoid temperature logs from boreholes located near mining shafts since they are usually affected by ground water flow resulting from mine water evacuation. Furthermore, the pumping can also lower the water-table by 100–150 m.

The geothermal data have already been published elsewhere. For data-set G, see Jessop et al. (1984) and references therein, and for data-set Q, see Mareschal et al. (1989) and Pinet et al. (1991).

Theoretical framework

For a homogeneous, isotropic, source-free half space, the temperature perturbation is a solution to the diffusion equation in one dimension with appropriate initial and boundary conditions (Carslaw and Jaeger, 1959):

$$\kappa \frac{\partial^2 T}{\partial z^2} = \frac{\partial T}{\partial t}, \qquad (1)$$

where κ is the thermal diffusivity of the rock, z is depth (positive downwards), and t is the time.

The present temperature perturbation $T(z)$in a semi-infinite solid with past surface temperature $T_0(t)$, where t is time before present, is given by (e.g. Vasseur et al., 1983):

$$T(z) = \frac{z}{2\sqrt{\pi\kappa}} \int_0^{\infty} T_0(t) t^{-3/2} \exp\left(-\frac{z^2}{4\kappa t}\right) \mathrm{d}t. \qquad (2)$$

This expression can be integrated for various surface temperature history model functions.

For a series of N instantaneous changes of the surface temperature T_k at times t_k before present, integration of Eq. 2 yields:

$$T(z) = \sum_{k=1}^{N} T_k \operatorname{erfc} \frac{z}{2\sqrt{\kappa t_k}} \qquad (3)$$

where erfc is the complementary error function. Such perturbations are strongly attenuated with depth.

In the Earth, the temperature perturbation is superimposed on the equilibrium temperature. The equilibrium temperature is extrapolated upward and the perturbation is determined as the difference between the measured temperature and the upward continuation of the deep temperature profile. The area between these curves represents the net heat absorbed by the ground and the shape of the perturbation is determined by the thermal history of the surface. This history can be determined by assuming a model and iterating until a satisfactory fit is obtained or, more generally, it can bè found directly by inversion (e.g. Vasseur et al., 1983; Lachenbruch and Marshall, 1986; Nielsen and Beck, 1989; Beltrami and Mareschal, 1991; Mareschal and Beltrami, 1992; Shen and Beck, 1991; Wang, 1992).

Direct model analysis

Each temperature log has been compared with the purely conductive response of a half space to a simple model of ground temperature. The model consists of a linearly increasing temperature over a finite time, preceded by an infinite time of constant temperature and followed by a time of constant temperature up to the time of logging, as illustrated in Fig. 2. There are five parameters in the model: the starting and ending surface temperatures, the times of beginning and end of the temperature increase, and the thermal diffusivity. However, since diffusivity and time always occur together as multiples, there are only four independent variables.

The only directly measurable quantities are the present surface temperature, the borehole temperatures and the thermal properties of the rock. Surface temperature is the result of a complex boundary-layer heat-transfer regime, which to date remains not well characterized. Thermal properties of rocks vary vertically and horizontally, but they are time independent, except where water saturation effects occur in the upper porous layers.

The thermal response of a half-space, initially at zero temperature, to linearly increasing temperature at the surface is given by (Carslaw and Jaeger, 1959, p. 63):

$$\Delta T(z, t) = 4sti^2 \operatorname{erfc}\left\{\frac{z}{2\sqrt{\kappa t}}\right\}, \qquad (4)$$

where s is the rate of change of surface temperature and i is the time integral of the error function. If we replace κt by a single variable w, this can be written as

$$\Delta T(z, t) = stf(z, w). \qquad (5)$$

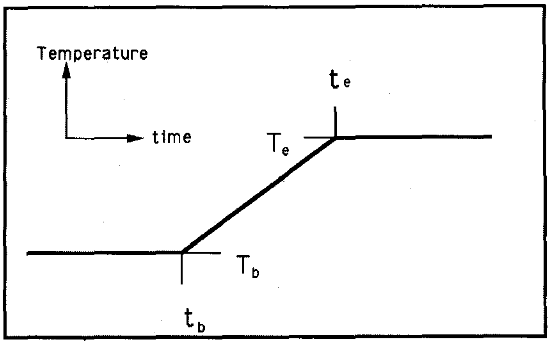

Fig. 2. Direct model scheme.

The final period of constant temperature is obtained by subtracting a second function of the same rate of temperature change

$$\Delta T = st_b f(z, w_b) - st_e f(z, w_e), \tag{6}$$

where subscript b denotes the beginning of the first function and of the temperature rise and e, the beginning of the second function and end of the temperature rise, as shown in Fig. 2. The rate of temperature change can therefore be written as

$$s = \frac{(T_e - T_b)}{(t_b - t_e)}. \tag{7}$$

Including the geothermal gradient, g, assumed constant over the depth interval examined, Eq. 6 can be written as:

$$T(z, t) = gz + \left\{ \frac{(T_e - T_b)}{(w_b - w_e)} \right\} \times \{ w_b f(z, w_b) - w_e f(z, w_e) \} \tag{8}$$

This version of the model shows that the five physical quantities may be combined into four independent variables.

Results from direct methods

Direct methods, using this the simple model of surface temperature have been applied to the analysis of the data described here. The model was iterated until a best-fit model, in terms of minimum rms, was found. The results are summarized in Fig. 3. It is clear that the warming signal is widespread in the area. There are only three sites exhibiting a cooling signal, and these sites are currently being investigated. This simple model may be framed in proper context by comparing the magnitude and timing of the inferred warming with longer time scales inversion.

The geographical distribution of temperature change is remarkably coherent, regardless of problems with individual sites. The map may be

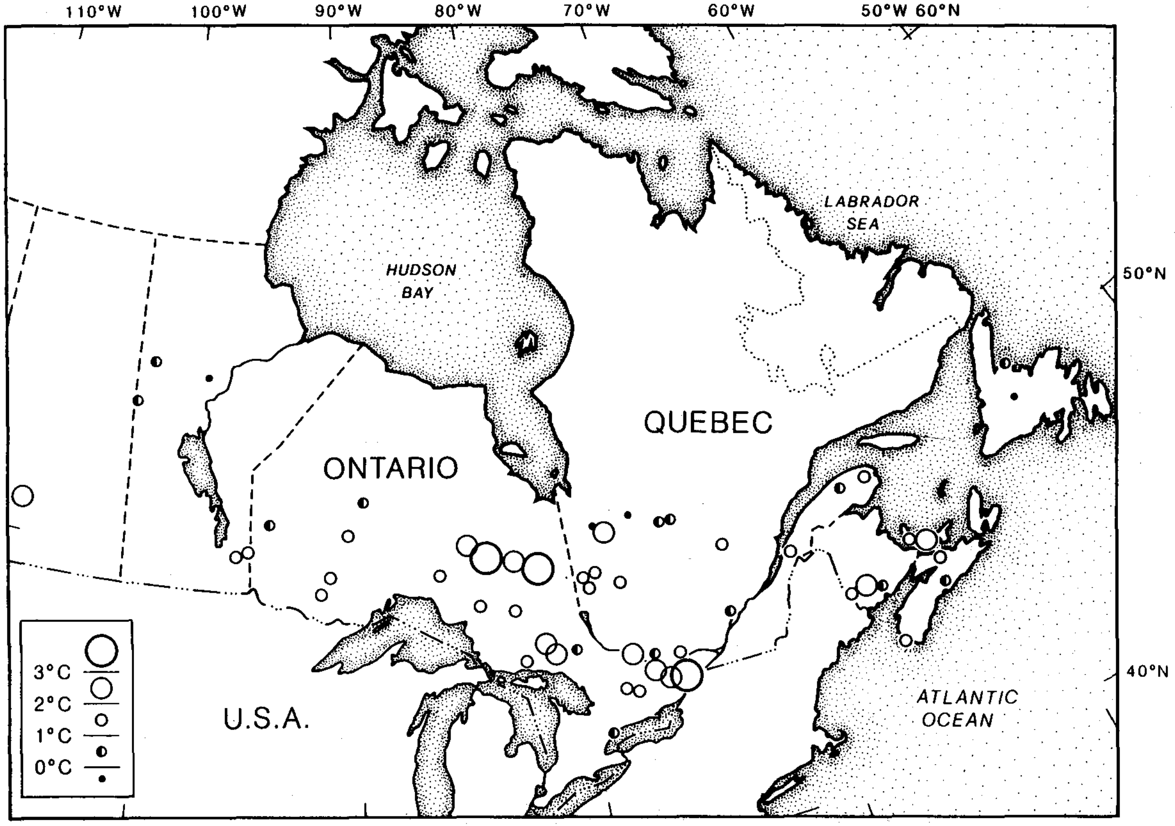

Fig. 3. Summary of direct method results for central and eastern Canada.

contoured with few points left as anomalies. The greatest changes, greater than 2°C, lie in an elongated zone running from the Ottawa Valley to the Kapuskasing area, and including the Sudbury area. To the east of this zone changes are generally between 1°C and 2°C in Québec, and to the west they fall to close to zero in northern Manitoba.

Inversion

The temperature perturbation at depth z, $T(z)$, can be written, taking into account the thermal conductivity variations, as the superposition of the equilibrium temperature and the perturbation $T_t(z)$ induced by the time dependent surface temperature condition:

$$T(z) = T_0 + q_0 R(z) + T_t(z) \qquad (9)$$

where T_0 is the equilibrium surface temperature, q_0 is the surface heat flow density and $R(z)$ is the thermal depth between the surface and depth z. The effect of heat production is small and has been neglected.

Because short-period variations are filtered out by the Earth, the surface temperature can be approximated by the average surface temperature over k time intervals of equal duration Δ, i.e:

$$T(t) = T_k (k-1)\ \Delta \le t \le k\Delta.$$

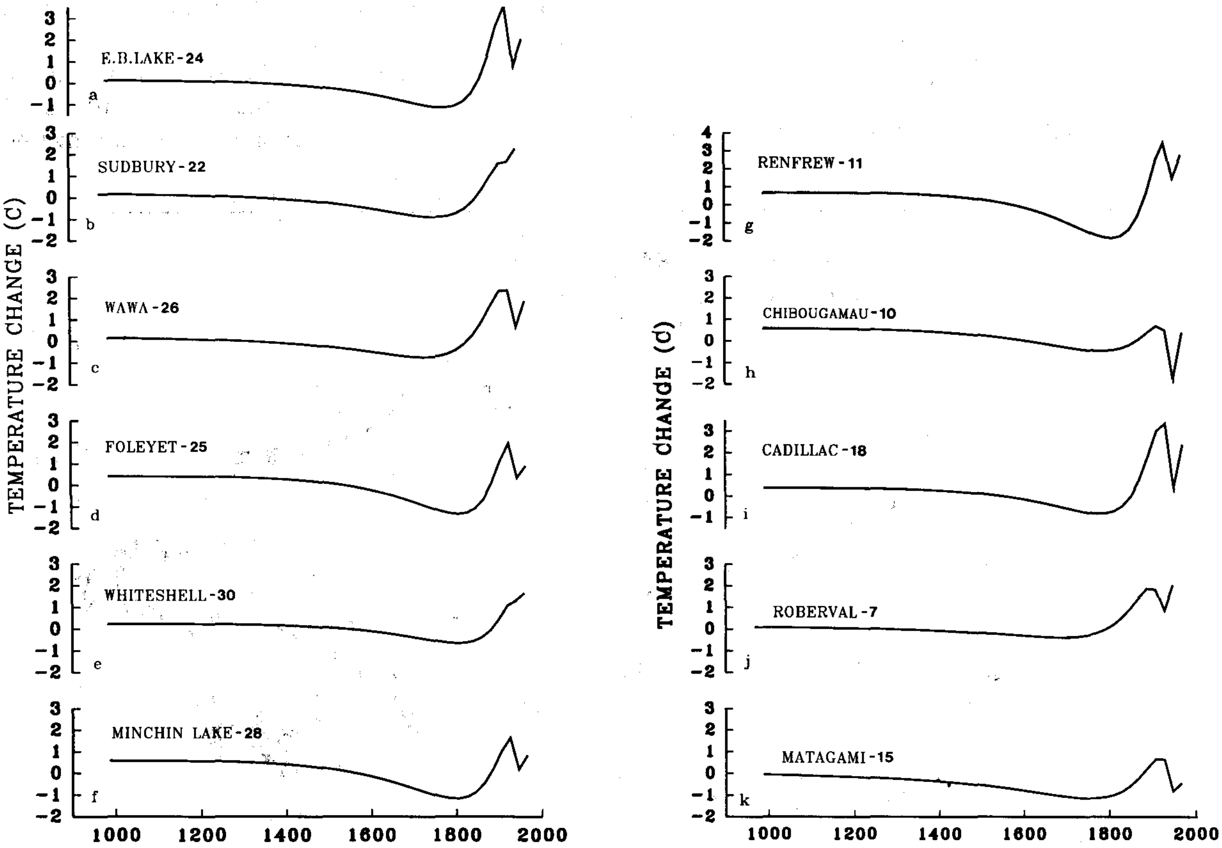

Fig. 4. Deep-borehole ground temperature histories for several cases over the studied regions. a. E.B. Lake, Ontario (G-300-3). b. Sudbury, Ontario (G-67-6). c. Wawa, Ontario (G-436-4). d. Foleyet, Ontario (G-437-3). e. Whiteshell, Manitoba (G-128-01). f. Minchin Lake, Ontario (G-016). g. Renfrew, Ontario (Q-88-1). h. Chibougamau, Québec (Q-90-9). i. Cadillac, Québec (Q-91-5). j. Roberval, Québec (G-06). k. Matagami, Québec (Q-87-47). l. Charlottetown, P.E.I. (G-341). m. Mc Dougal P.E.I. (G-345). n. Lynn Lake, Manitoba (G-149-1). o. Flin-Flon, Manitoba (G-136-1). p. Baie Verte, Newfoundland (G-152-1). Numbers besides name indicate Fig. 1 map codes.

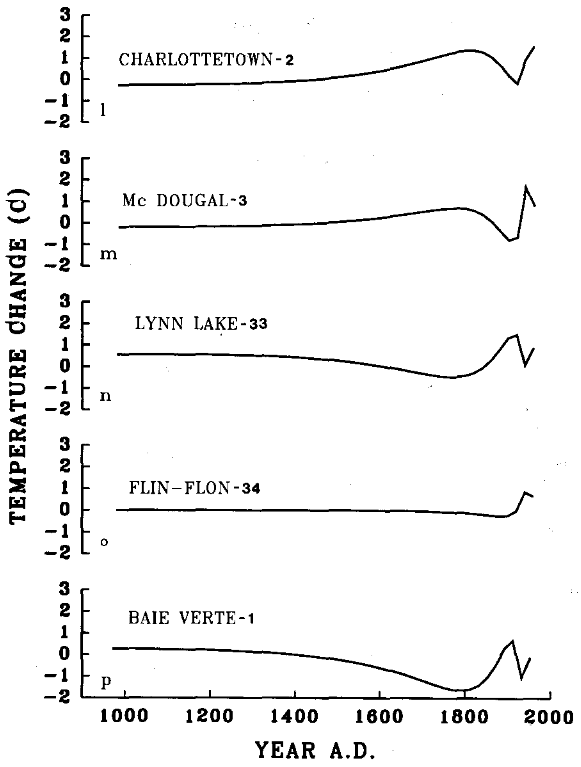

Fig. 4 (continued).

Equation 9 can then be written as:

$$\Theta_j = A_{jk} X_i \tag{10}$$

where Θ_j is the measured temperature at depth z_j, X_i is a vector containing the unknowns $\{T_o, q_o, T_1, \ldots, T_K\}$ and A_{jk} is a matrix, each row of which contains 1 in the first column, the thermal resistance to depth z_j in the second column, and the K elements formed by evaluating the difference between complementary error functions at times $t_{k-1} = (\text{k-1})\,\Delta$ and $t_k = k\Delta$:

$$A_{jk+2} = \operatorname{erfc}\left\{\frac{z_j}{2\sqrt{\kappa t_{k-1}}}\right\} - \operatorname{erfc}\left\{\frac{z_j}{2\sqrt{\kappa t_k}}\right\} \tag{11}$$

The above yields an underdetermined system of linear equations which can be solved by singular value decomposition (SVD) (Lanczos, 1961; Jackson, 1972; Menke, 1989).

Although it is possible to deal with a layered conductivity following the approach above, this is seldom useful considering the quantity and quality of the existing thermal conductivity data. Indeed, in a crystalline environment, horizontal lithological and thus horizontal conductivity layering is unusual. The horizontal thermal conductivity variations may be as large as vertical variations and result in uniform bulk conductivity of the rock at large scales. Tests of this inversion regarding thermal conductivity variations with depth have been carried out and are presented in Shen et al. (1992, this issue). The effect of internal heat generation has been ignored for boreholes of less than 600 m when rates of internal heat generation are low and typical of Shield conditions (i.e. $< 1\ \mu\text{W/m}^3$). This effect has been taken into consideration for the analysis of deeper boreholes. For the case of G-18 (Wedgeport) which presents a larger than usual heat generation rate (Lewis and Bentkowski, 1988), this has been ignored since the borehole is only 260 m deep.

Different inversion techniques have been applied to this problem (e.g. Vasseur et al., 1983; Shen and Beck, 1983; Nielsen and Beck, 1989; Wang, 1992; Shen and Beck, 1991). The analysis reported here is based on the generalized inverse for a linear underdetermined system of equations which has been described by Mareschal and Beltrami (1992). The inversion scheme used in this analysis performs well for the quality of the existing data. Its robustness has been examined in Beck et al. (1992) and Shen et al. (this issue).

The model chosen (unless stated otherwise) for the ground temperature history in the inversion consists of 50 equally spaced time intervals and the singular-value cutoff has been set at 0.025. The singular-value cutoff restricts the resolution but improves the stability of the solution; it reflects the trade off between variance and resolution (Jackson, 1972). The standard deviation of the estimated GTH given in some of the figures, represent the stability of the solution with respect to a data random noise level of 0.02 K (Mareschal and Beltrami, 1992).

Analysis and results from inversion

Figure 4 shows several solutions found for deep-boreholes in Ontario, Manitoba, Québec and Newfoundland (see Table 1). The qualitative agreement between solutions is remarkable. All sites show the post-industrial warming and the LIA cold period. The signal due to the LIA was previously inferred by Cermak (1971) from the analysis of two boreholes (although with poor resolution), and in four boreholes from the same area by Nielsen and Beck (1989). Recently, the LIA signature has been independently inferred by Shen and Beck (this issue) and Wang (1992), for boreholes in the same area.

TABLE 1

Borehole identification number, coordinates, map identification number and equilibrium surface temperature for the GTHs shown im the figures

Number	Name	Latitude	Longitude	Map number	T_{eq}(°C)
G-152-1	Baie Verte	49-54.3N	56-03.3W	1	4.9
G-341	Charlotteto	46-15.7N	63-08.3W	2	5.8
G-345	Macdougall	46-30.5N	63-56.5W	3	6.5
G-96	Sunnybank	48-51.5N	64-40.7W	4	4.2
G-18	Wedgeport	43-45.4N	66-00.0W	5	7.1
G-144G	Tracy	45-41.0N	66-41.0W	6	4.7
G-6	Roberval	48-31.8N	72-15.2W	7	4.4
Q-89-28	Crevier	49-28.0N	72-46.4W	8	3.3
Q-87-05	St.Ellie	46-29.3N	72-57.3W	9	6.4
Q-90-09	Chibougamau	49-53.9N	74-10.2W	10	3.8
Q-88-01	Renfrew	45-25.4N	76-42.3W	11	6.5
Q-89-18	Kaladar	42-03.1N	77-10.8W	12	6.9
Q-87-09	Val d'Or	48-06.0N	77-33.3W	13	3.7
Q-89-10	Limerick	44-52.4N	77-43.3W	14	5.7
Q-87-47	Matagami	49-42.7N	77-44.3W	15	3.4
Q-88-19	Cordova	44-32.1N	77-47.1W	16	6.9
Q-89-21	Cardiff	45-00.4N	78-02.1W	17	6.3
Q-91-05	Cadillac	48-15.1N	78-26.2W	18	3.6
G-156	Launay	48-38.9N	78-26.5W	19	3.8
G-89-05	Salerno	44-51.4N	78-38.1W	20	6.3
Q-88-11	Belleterre	47-24.0N	78-24.6W	21	4.0
Q-88-10	Belleterre	47-24.0N	78-42.6W	21	4.0
Q-88-12	Belleterre	47-24.1	78-42.6W	21	3.9
Q-88-13	Belleterre	47-24.1	78-42.7W	21	4.1
G-67-6	Sudbury	46-30.9N	81-05.1W	22	5.7
G-67	Onaping	46-39.N	81-18.2W	23	5.5
G-300-3	E. Bull L.	46-25.5N	82-13.1W	24	5.5
G-437-3	Foleyet	47-56.4N	82-24.6W	25	3.9
G-436-1	Wawa	48-18.1N	84-25.8W	26	3.8
G-436-4	Wawa	48-18.1N	84-25.8W	26	3.6
G-84-2	Manitouwad	49-11.2N	85-48.6W	27	3.0
G-84-1	Manitouwad	49-10.6N	85-50.9W	27	3.2
G-84-3	Manitouwad	49-11.1N	85-50.9W	27	3.2
G-84-4	Manitouwad	49-11.0N	85-50.9W	27	3.7
G-84-6	Manitouwad	49-10.8N	85-50.9W	27	3.5
G-84-7	Manitouwad	49-10.8N	85-50.9W	27	3.1
G-16	Minchin L.	50-42.7N	90-28.8W	28	3.8
G-133	Atikokan	48-54.1N	91-41.8W	29	4.2
G-128-1	Whiteshell	50-12.0N	95-55.0W	30	4.3
G-138	Thompson	55-43.5N	97-46.0W	31	1.0
G-137-1	Snow Lake	54-53.6N	99-57.9W	32	2.0
G-149-1	Lynn Lake	56-47.4N	101-06.6W	33	0.5
G-150-1	Fox Lake	56-37.9N	101-39.0W	33	1.3
G-136-1	Flin Flon	54-38.6N	102-02.3W	34	1.9
G-442-3	Riverhurst	50-52.7N	106-51.7W	35	3.9

The timing of the minimum ground temperature during the LIA does not change significantly between most of the solutions found from usable boreholes; this is well illustrated by the solutions shown.

Since the inversion of geothermal data for ground temperature history determination is a non-unique problem, care must be taken to obtain a "reasonable" estimate of the temperature minimum during the LIA in particular, and of surface temperature changes in general. A necessary condition is to assume a model GTH that covers a time span sufficiently long (relative to the depth of the borehole), i.e. ~ 5000 yr for a 600 m temperature log. Shorter model histories would increase the inferred temperature changes by distributing the ground heat loss/gain in a short time span (Shen et al., this issue). A rough estimate of the resolving power of the data can be obtained by calculating the maximum temperature perturbation due to a change in T degrees, during a time interval ∂t, starting t years ago. This is given by: $T_{\max} = 0.24\ T\partial t/t$. If the detection threshold is 0.05 K, $T\partial t/t = 0.21$. That is, a perturbation can be detected only if its duration is at least 20% of the time of occurrence.

Most boreholes in the Atlantic provinces yield solutions (only two shown here) exhibiting significant *warming* of the ground starting some 500 years ago, at the time of the onset of the LIA. This peculiarity of GTHs in the Atlantic Provinces might be explained by an increase in snow cover for the fall and spring months during the LIA. Indeed, it has been well documented that the mean annual ground temperature is significantly higher than the air temperature because of the insulating effect of the snow (e.g. Geiger, 1965; Tuller and Chilton, 1972; Smith, 1975). The cooling of the air might have been masked by a warming of the ground due to increased snow cover. It must be pointed out that proxy climatic records near this area indicate definitely the existence of the LIA as well as an increase in precipitation during this period (Gajewski, 1988; Bernabo, 1981). More data need to be examined to clarify this phenomenon.

It is apparent that the magnitude of the LIA maximum cooling is large in Newfoundland and smaller in northern Manitoba, with the rest of the country showing cooling of more or less the same magnitude (~ 1°C). The post-industrial warming appears clearly reduced in Newfoundland and at two sites in northern Québec (Matagami and Chibougamau). These differences are being investigated.

Figure 5 shows several solutions obtained for a number of boreholes with depths between 150 and 300 m. The ground temperature model consists of a series of fifty 10-yr steps and the singular value cutoff remains at 0.025. The recovered features of the solutions agree well with the deeper borehole solutions. These shallower boreholes can detect the warming relative to the LIA but are not deep enough to be sensitive to the climatic history preceding the LIA minimum.

In order to obtain robust solutions, site averaging was performed assuming that after thermal conductivity and other corrections have been carried out, the temperature perturbation in the subsurface is entirely of climatic origin; if this is the case and the surface conditions between boreholes do not differ significantly, it is reasonable to assume that the climatic change responsible for the temperature anomalies is the same over the whole area. Then, the temperature perturbation for all boreholes at a site can be inverted simultaneously, provided that the temperature logs have similar depths and sampling intervals, and that measurements were made at roughly the same time. If measurements were made many years apart and accurate data are available, then the inversion scheme can be easily modified to account for the time rate of change of the subsurface signal. This averaging procedure is better than simply averaging the solutions since it increases the amount of data and thus the stability of the solution and if the same climatic signal is indeed recorded it improves the signal to noise ratio, provided that the noise is random.

Figure 6 shows an example of site averaging. The data correspond to four boreholes measured at Belleterre (Quebec); each borehole was inverted individually (*a*–*d*) for a series of fifty 20-yr steps and then all four were inverted simultaneously (*e*) for the same ground temperature model. It can be seen that the stability of the average

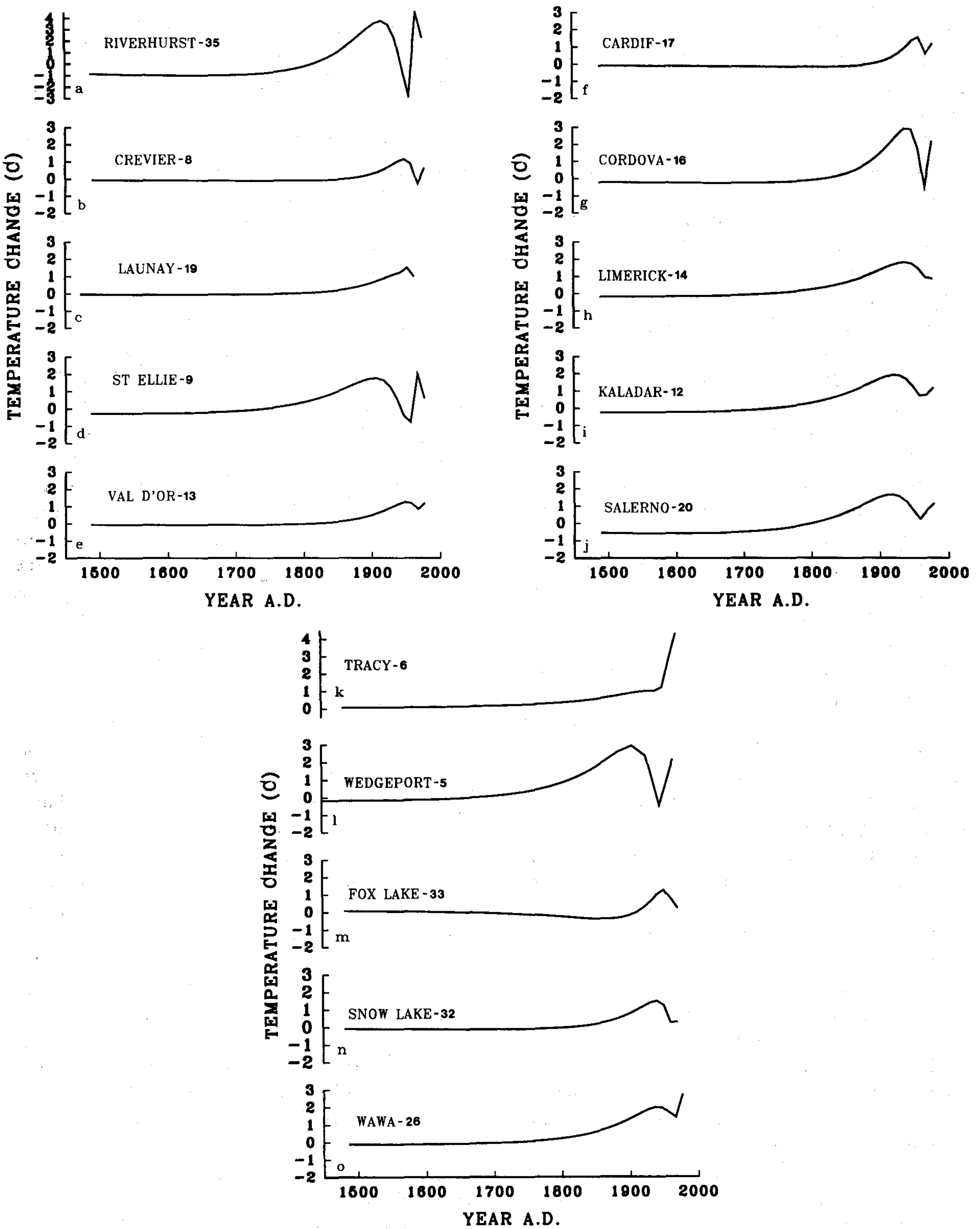

Fig. 5. Shallow-borehole ground temperature histories for several locations in Canada. a. Riverhurst, Saskatchewan (G-442-3). b. Crevier, Québec. c. Launay, (G-156) Québec. d. St Ellie, Québec. e. Val d'Or, Québec. (Q-87-09). f. Cardif, Ontario (Q-89-21). g. Cordova Mines, Ontario (Q-88-19). h. Limerick, Ontario (Q-89-10). i. Kaladar, Ontario (Q89-18). j. Salerno, Ontario (Q-89-5). k. Tracy, New Brunswick (G-144). l. Wedgeport, (G-18). m. Fox Lake, Manitoba (G-150-1). n. Snow Lake, Manitoba (G-137-1). o. Wawa, Ontario (G-436-1). Numbers besides name are map codes.

solution is greatly improved, according to the standard deviation of the estimated parameters. These borehole temperature logs have the same sampling densities and similar depths, ensuring that the solution is not biased towards the profile with smaller sampling interval. These data requirements largely reduce the number of *currently available* temperature logs usable for site or regional average GTH determination.

Figure 7 shows several site-average solutions found by the above-described simultaneous inversion. Most of the site averages show GTHs with the same characteristics over a large area; this suggests that the same forcing factors have controlled the subsurface temperature over the whole area. Some of the differences in site average GTH might be due to local effects caused by microclimates; regional averages of these sites might help to smooth out a larger scale GTH.

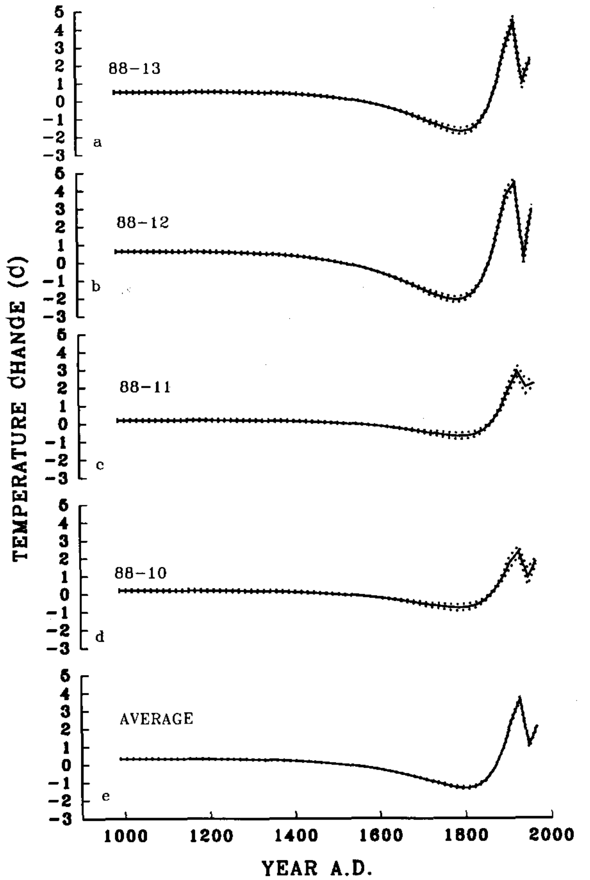

Fig. 6. Example of site averaging. a. Solution for single borehole 88-13 at Belleterre, Québec. b–d. Similar solutions for boreholes 88-12, 88-11, 88-10, respectively. e. Ground temperature history obtained from the simultaneous inversion of the four above temperature logs. The dashed curves represent the standard deviation of the estimated GTHs for an assumed 0.02 K data noise level.

To find a suitable solution at a regional scale the same concept can be used as long as the individual profiles and solutions do not indicate drastic qualitative differences in GTH. This situation is more delicate than site averaging since the climate has been documented to change over scales of a few hundred kilometers owing to the effects of microclimates. Since the area of study is vast we have attempted to reduce the individual climatic histories to regional averages.

Figure 8 shows a deep-borehole regional solution for Ontario obtained from the simultaneous inversion of five temperature logs. Only deep boreholes were used for the estimation of the regional solution as long as shallow boreholes in the same sites of the region, if they exist, do not contradict the GTH obtained from deep boreholes. This can be verified by examining the time rate of change of the temperature history or by comparing the GTHs obtained from analysis for the same length of the temperature logs (see Appendix A). Other regions do not have a sufficient number of deep-borehole temperature logs to yield an unequivocal average solution.

Finally, Fig. 9 shows two solutions found from very deep-borehole (> 800 m) temperature logs. The ground surface temperature model used consists of two hundred 25-yr steps and the singular value cutoff eigenvalue was set to 0.025. The GTHs include earlier warm periods which might be associated with the climatic optimum. Additional data from very deep boreholes are needed to clarify the timing of this variation. However, its existence confirms that the Earth's climate is subjected to variability on many time scales. Independent analyses of deep boreholes in Canada (Wang, 1992), and in France (Mareschal and Vasseur, this issue) have also identified a similar warm event.

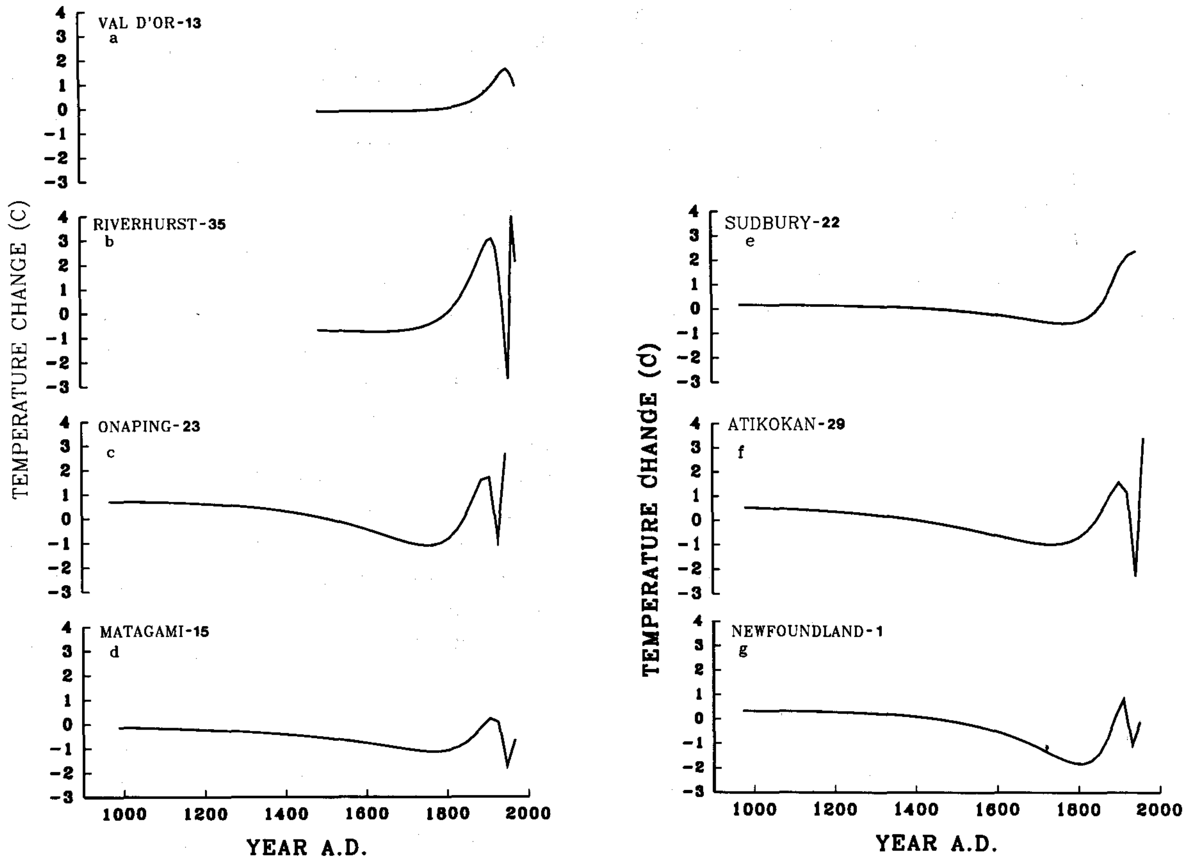

Fig. 7. Examples of site averages. a. Val d'Or, Québec (2). b. Riverhurst, Saskatchewan (4). c. Onaping, Ontario (2). d. Matagami, Québec (4). e. Sudbury, Ontario (2). f. Atikokan, Ontario (2). g. Baie Verte, Newfoundland (2). The number in parenthesis indicate the number of temperature logs used in the simultaneous inversion. Numbers besides name are map codes.

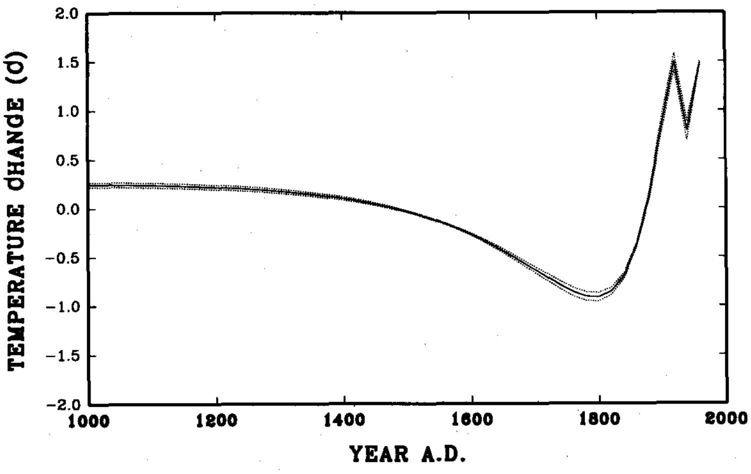

Fig. 8. Estimated regional ground temperature history for eastern Canada (region between 96°W and 80°W and 46°N and 50°N). This solution was obtained from the simultaneous inversion of five temperature profiles in the area. Other regions do not have a sufficiently large number of deep boreholes as to make solutions unequivocal. Dashed lines represent the standard deviation for an assumed 0.02 K data noise level.

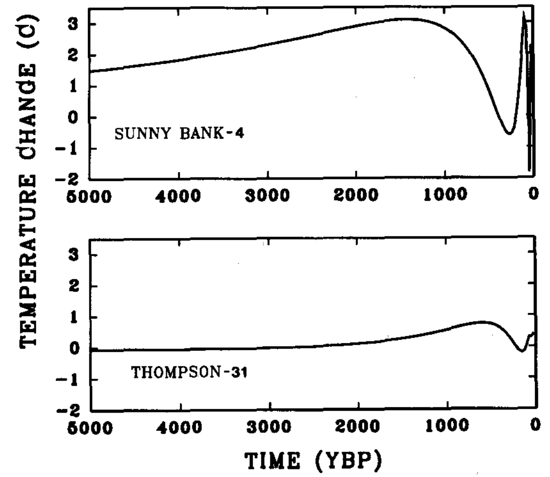

Fig. 9. Ground temperature history for very deep boreholes. a. GTH for Sunny Bank, Québec (G-96) and b. GTH for Thompson, Manitoba (G-138).

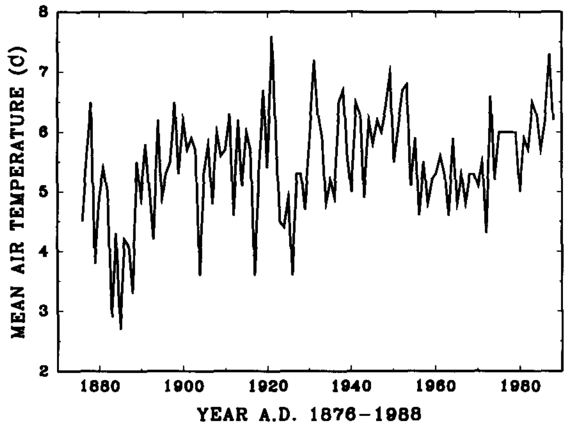

Fig. 10. Surface air temperature annual averages for longest meteorological station (Parry Sound) in eastern Canada. The record indicates an increasing air temperature trend of about 1°C in one century. The cooling period around the 1950's is clearly identifiable (Data from Environment Canada).

Discussion

Comparison with meteorological records and proxy data

The features in the solutions agree well with the meteorological records for the area (Diaz and Bradley, 1990) and with Fig. 10, showing the annual mean surface air temperature for the meteorological station with the longest record in eastern Canada (Parry Sound). The cooling period around 1950 is present in the regional GTH as well as in the air temperature record. The total air temperature increase, according to this station, is about 0.9°C in about 100 years, and agrees with the magnitude (~ 1°C) estimated for central and eastern Canada from geothermal measurements (see Fig. 8).

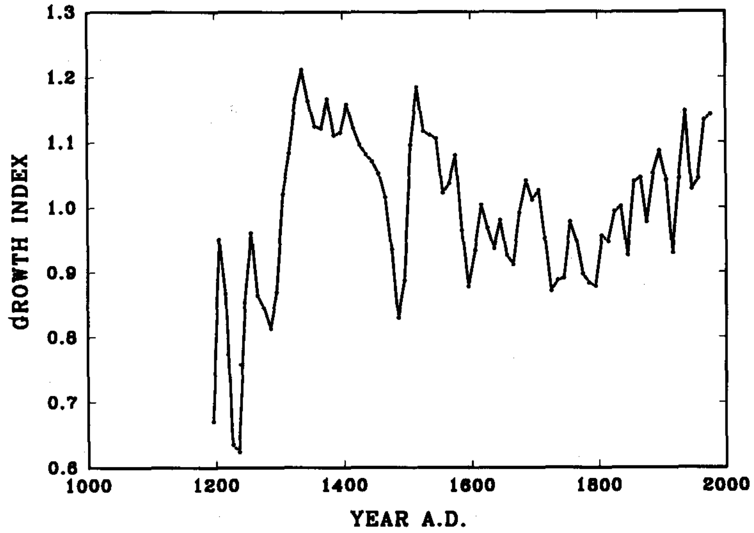

Fig. 11. 802-year dendrochronological record at Rouyn. Shown is the 20-yr running mean with 11 yr shift. The raw data has been normalized and corrected for the effects of forest fires (Archambault and Bergeron, 1992).

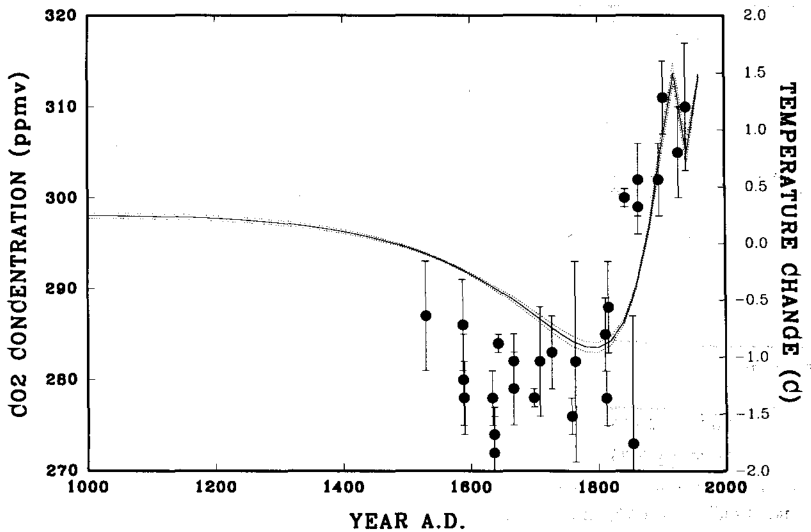

Fig. 12. Average regional ground temperature history (solid line) and atmospheric concentration of carbon dioxide as reported form a Greenland ice core (Wahlen et al., 1991). The dashed lines represent the standard deviation of the estimated model parameters for the solution found. There is no significant change in the atmospheric concentration of CO_2 prior to 1810 A.D..

Comparison of GTHs with dendrochronological records

The estimated GTHs are in qualitative agreement with dendrochronological records for the area (Archambault and Bergeron, 1992). Figure 11 shows the 20-yr running mean with 10 yr shift for the tree-ring index of a 800-yr long dendrochronological time series at Rouyn (Québec) (48° 28′N, 79° 17′W); the signal for the LIA corresponds well to the timing found from geothermal measurements for this event, although the resolution of the GTH before 1500 A.D. is poor. To date no attempt has been made to reconstruct the long range air temperature history from these data. Other dendrochronological data for northern North America have been used for temperature history reconstruction by Jacoby and D'Arrigo (1989) and D'Arrigo and Jacoby (1992). Their reconstructed temperature histories show a cold period with a minimum in the middle 1800s and the subsequent warming (~ 1°C) in agreement with the northern Manitoba GTHs presented above. These temperature reconstructions were obtained from tree-ring data at seven sites, six of them in northern North America and they are expected to represent no more than this area. The fact that these temperature reconstructions are in agreement with the northern GTH and that the southern GTH agrees with dendrochronological data in Québec suggest that there might have been different patterns of the LIA in Canada (Beltrami and Mareschal, 1992).

Correlation with concentration of atmospheric CO_2

The average GTH (Fig. 12) is also correlated with the concentration of atmospheric carbon dioxide as reported in a Greenland ice core (Wahlen et al., 1991). Furthermore, the reversal of the minimum cooling during the LIA (~ 1800 A.D.) coincides with the increase in the concentration of atmospheric CO_2 (~ 1810 A.D.). The latter correlation, as it stands, does not permit the establishment of a cause–effect relation. Further atmospheric CO_2 concentration data are needed to substantiate the apparent absence of significant change on the concentration of this greenhouse gas in the atmosphere during the full extent of the Little Ice Age. One would expect that if the atmospheric CO_2 concentration declined during the LIA, it would have been higher before 1500 A.D.; otherwise, alternative mechanisms might be involved in the global redistribution of heat.

Conclusions

A significant post-industrial warming of the ground has been detected over central and eastern Canada. Furthermore, this work confirms the existence of a cold period coinciding with the LIA cold event documented mostly in Europe and in some parts of North America (Grove, 1988). The inferred ground temperature variations are accompanied by changes in the concentration of atmospheric carbon dioxide; it is not possible to determine a cause–effect relation between variations in this greenhouse gas and the observed temperature fluctuations.

These results confirm the usefulness of geothermal data to reconstruct climatic histories on the continents. Other effects can interfere with the isolation of the ground temperature signal, but a careful selection of the borehole temperature profiles and a study of the surface conditions and its changes, can eliminate most of the known sources of noise. In other words, it is possible to obtain a climatic signal from suitable boreholes.

Furthermore, since GTH inferred from geothermal measurements acts as an integrator primarily of the effects of surface air temperature and the precipitation regime, it may be better suited as an indicator of climatic change than air temperature records alone.

Acknowledgements

We are grateful to Dr. Yves Bergeron for making available to us their tree-ring data. We thank Drs. P.Y. Shen and Kelin Wang for discussions while this work was carried out, and Dr. T. Lewis and an anonymous referee for constructive comments. J.C.M. is grateful for the generous and continuous support of the Natural Sciences and Engineering Research Council (Canada) and the fonds pour la Formation de Chercheurs et l'Aide à la Recherche (Québec). H.B. received fellowships from PFACC and the Chaire de Recherche en Environnement (HydroQuébec-NSERC-UQAM).

Appendix A

Comparing GTH from temperature logs for boreholes of different depth.

Assessment of the consistency of the solutions obtained from temperature logs of different lengths in a site or region, can be achieved by performing the analysis for the same thermal depth so as to fix the reference temperature at more less equal magnitude (Chapman, 1991, pers. comm.). Figure A1 shows a set of solutions for Minchin Lake (NW Ontario) for different "lengths" of the log. The equilibrium temperature has been arbitrarily taken as given by the extrapolation of the Bullard plot in the deepest 50 m of the logs and the temperature perturbation calculated as usual. Once this analysis has been done it is easier to compare these solutions with shallower boreholes from far apart regions to search for regularities. For example, the solu-

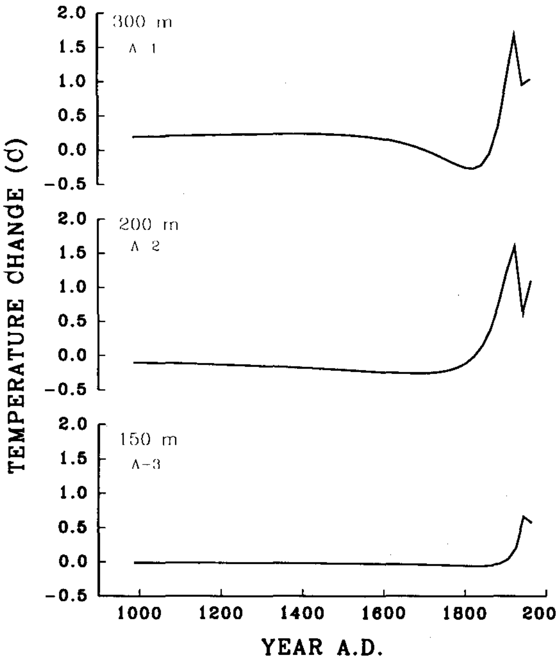

Fig. A-1. Ground temperature history for Minchin Lake for a temperature log of 300 m. Equilibrium temperature was found from a linear regression in the deepest 50 m. A-2. Ground temperature history for Minchin Lake for a temperature log of 200 m. A-3. Ground temperature history for Minchin Lake for a temperature log of 100 m. See Fig. 4f for Minchin Lake full temperature log analysis.

tion for Minchin Lake (Fig. A2), truncated to the same thermal depth as Val d'Or (Fig. 5e), presents the same features as the latter, although these boreholes are some 1000 km apart and at different latitudes. This shows that a minimum borehole depth is required to appropriately assess the magnitude of the post industrial warming.

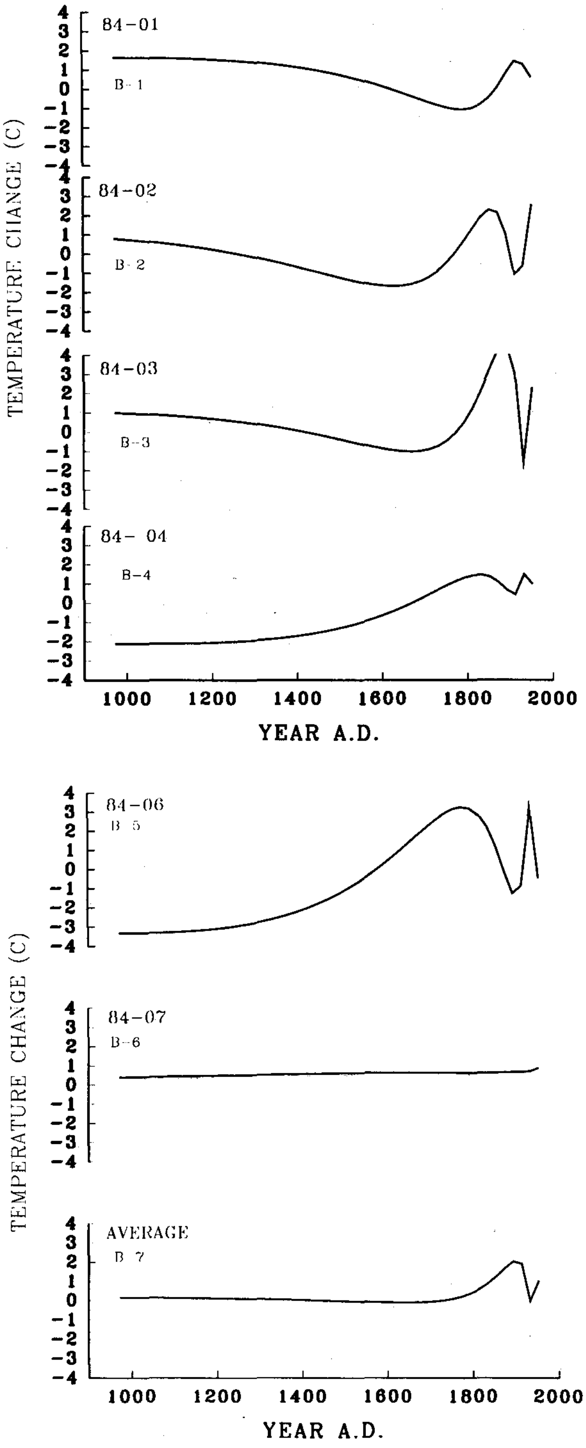

Fig. B1-7. GTHs obtained by inversion of temperature perturbation for six borehole temperature logs at one site (Manitouwadge, Ontario). The inversion of individual temperature logs yield diverse solutions and the magnitudes of the temperature changes vary prohibitively. This illustrates the possible problems associated with attempts to determine a significant solution for a site for a single temperature log. The numbers on the figures are borehole identification.

Appendix B

Conflicting data: an example

Large temperature perturbation discrepancies can exist between boreholes in the same site. Figures B1-6 illustrate the resulting GTHs for six boreholes temperature logs at the same site (Manitouwadge, Ontario). Although, the solutions for the climatic history from some individual boreholes yields qualitatively similar solutions, the magnitude of the temperature changes inferred is inconclusive. An attempt to invert simultaneously these temperature logs do show recent warming (Fig. B7), but the temperature change inferred drops quickly to near zero; this apparent lack of signal is due to the large spread of the temperature perturbations in the subsurface. This, again, brings attention to the lack of characterization of the heat transfer regime through the air ground interface at the Earth' surface, and the dangers involved in interpreting a solution obtained from a single temperature log as representative of the climatic changes in an area.

References

Archambault, S. and Bergeron, Y., 1992. A 802-year tree-ring chronology from Quebec boreal forest. Can. J. For. Res., 22: 674–682.

Beck, A.E., 1977. Climatically perturbed temperature gradients and their effects on regional and continental heat-flow means. Tectonophysics, 41: 17–39.

Beck, A.E., Shen, P.Y., Beltrami, H., Mareschal, J.C., Safanda, J., Sebagenzi, S., Vasseur, G. and Wang, K., 1992. A comparison of 5 different analyses of interpreting 5 data sets. Palaeogeogr., Palaeoclimatol., Palaeoecol.(Global Planet. Change Sect.), 98: 101–112.

Beltrami, H. and Mareschal, J.C., 1991. Recent warming in Eastern Canada: evidence from geothermal measurements. Geophys. Res. Lett., 18: 605–608.

Beltrami, H. and Mareschal, J.C., 1992. Ground temperature changes in Eastern Canada: Borchole temperature evidence compared with proxy data. Terra Nova, in press.

Bernabo, J.C., 1981. Quantitative estimates of temperature changes over the last 2700 years in Michigan pollen data. Quat. Res., 15: 143–159.

Birch, F., 1948. The effects of Pleistocene climatic variations upon geothermal gradients. Am. J. Sci., 246: 729–760.

Backwell, D.D., Steele, J.L. and Brott, C.A., 1980. The terrain effect on terrestial heat flow. J. Geophys. Res., 85: 4757–4772.

Carslaw, H.S. and Jaeger, J.C., 1959. Conduction of Heat in Solids. Oxford Univ. Press, 2nd ed., 510 pp.

Cermak, V., 1971. Underground temperature and inferred climatic temperature of the past millennium. Palaeogeogr., Palaeoclimatol., Palaeoecol., 10: 1–19.

Chisholm, T.J. and Chapman, D.S., 1992. Climate change inferred from analysis of borehole temperatures: an example from western Utah. J. Geophys. Res., in press.

D'Arrigo, R.D. and Jacoby, G.C., 1992. Dendrochronological evidence from northern North America. In: R.S. Bradley and P.D. Jones (Editors),Climate since A.D. 1500. Routledge, London.

Diaz, H.F. And Bradley, R.S., 1990. Analysis of long-term climatic records at high elevation in the northern hemisphere. In: Int. Symp. Clima Locarno 1990, September 1990.

Elsner, J.B. and Tsonis, A.A., 1991. Comparison of observed northern hemisphere surface air temperature records. Geophys. Res. Lett., 18: 1229–1232.

Geiger, R., 1965. The Climate Near the Ground. Harvard Univ. Press, Cambridge, MA, 611 pp.

Gajewski, K., 1988. Late Holocene climate changes in eastern North America estimated from pollen data. Quat. Res., 29: 255–262.

Ghil, M. and Vautard, R., 1991. Interdecadal oscillations and the warming trend in global temperature time series. Nature, 350: 324–327.

Grove, J.M., 1988. The Little Ice Age. Methuen, London, 498 pp.

Hansen, J. and Lebedeff, S., 1987. Global trends of measured air-surface temperature. J. Geophys. Res., 92: 13,345–13,372.

Jackson, D.D., 1972. Interpretation of inaccurate, insufficient, and inconsistent data. Geophys. J.R. Astron. Soc., 28: 97–110.

Jacoby, G.C. and D'Arrigo, R., 1989. Reconstructed Northern Hemisphere annual temperature since 1671 based on high-latitude tree-ring data from North America. Clim. Change, 14: 39–59.

Jessop, A.M., Lewis, T.J. Judge, A.S., Taylor, A.E. and Drury, M.J., 1984. Terrestial heat flow in Canada. Tectonophysics, 103: 239–261.

Jones, P.M., Wigley, M.L. and Wright, P.B., 1986. Global temperature variations between 1861 and 1984. Nature, 322: 430–434.

Karl, T.R., Tarpey, J.D., Quayle, R.G., Diaz, H.F., Robinson, D.A. and Bradley, R.S., 1989. The recent climate record: what it can and cannot tells us. Rev. Geophys., 27: 405–430.

Lachenbruch, A. and Marshall, B.V., 1986. Changing climate: geothermal evidence from permafrost in the Alaskan Arctic. Science, 234: 689–696.

Lanczos, C., 1961. Linear Differential Operators. Van Nostrand, New York, 564 pp.

Lewis, T.J. and Bentkowski, W., 1988. Potassium, uranium and thorium concentrations of crustal rocks: a data file. Geol. Surv. Can. Open File Rep., 1744.

Mareschal, J.C., Pinet, C., Gariépy, C., Jaupart, C., Bienfait, G., Dalla Coletta, G., Jolivet, J. and Lapointe, R., 1989. New heat flow density and radiogenic heat production data in the Canadian shield and the Quebec Appalachians. Can. J. Earth Sci., 26: 845–852.

Mareschal, J.C. and Beltrami, H., 1992. Evidence for recent warming from perturbed geothermal gradients: examples from Eastern Canada. Clim. Dyn., 6: 135–143.

Mareschal, J.C. and Vasseur, G., 1992. Ground temperature history from two deep boreholes in Central France. Palaeogeogr., Palaeoclimatol., Palaeoecol. (Global Planet. Change Sect.)., 98: 185–192.

Menke, W., 1989. Geophysical Data Analysis: Discrete Inverse Theory. (Int. Geophys. Ser., 45). Academic Press, San Diego, 289 pp.

Nielsen, S.B. and Beck, A.E., 1989. Heat flow density values and paleoclimate determined from stochastic inversion of four temperature–depth profiles from the Superior Province of the Canadian shield. Tectonophysics, 164: 345–359.

Pinet, C., Jaupart, C., Mareschal, J.C., Gariépy, C., Bienfait, G. and Lapointe, R., 1991. Heat flow and structure of the lithosphere in Eastern Canada. J. Geophys. Res., 96: 19,941–19,963.

Shen, P.Y. and Beck, A.E., 1983. Determination of surface temperature history from borehole temperature gradients. J. Geophys. Res., 88: 7385–7493.

Shen, P.Y. and Beck, A.E., 1991. Least squares inversion in borehole temperature measurements in functional space. J. Geophys. Res., 96: 19,965–19,979.

Shen, P.Y. and Beck, A.E., 1992. Paleoclimate change and heat flow density inferred from borehole temperature data in the Superior Province of the Canadian shield. Palaeogeogr., Palaeoclimatol., Palaeoecol. (Global Planet. Change Sect.), 98: 143–165.

Shen, P.Y., Wang, K., Beltrami, H. and Mareschal, J.C., 1992. A comparative study of inverse methods for estimating climatic histories from borehole temperature data. Palaeogeogr., Palaeoclimatol., Palaeoecol. (Global Planet. Change Sect.), 98: 113–127.

Smith, M.W., 1975. Microclimatic influences on ground temperatures and permafrost distribution, Mackenzie Delta, Northwest Territories. Can. J. Earth Sci., 12: 1421–1438.

Tuller, S.E. and Chilton, R., 1972. Patterns of maximum and minimum air and soil temperatures near a forest edge. Arch. Meteorol. Geophys. Biokl., B20: 285–298.

Vasseur, G., Bernard, P., Van de Meulebrouck, J., Kast, Y. and Jolivet, J., 1983. Holocene paleotemperatures deduced from geothermal measurements. Palaeogeogr., Palaeoclimatol., Palaeoecol., 43: 237–259.

Wahlen, M., Allen, D., Deck, B. and Herchenroder, A., 1991. Initial measurements of CO_2 concentrations (1530 to 1940) in air occluded in the GISP 2 ice core from central Greenland. Geophys. Res. Lett., 18: 1457–1460.

Wang, K., 1992. Estimation of ground temperature history from borehole temperature data. J. Geophys. Res., 97: 2095–2106.

Willmott, C.J., Robeson, S.M. and Feddema, J.J., 1991. Influence of spatially variable instrument networks on climatic averages. Geophys. Res. Lett., 18: 2249–2251.